analytical chemistry

Article

Cite This: Anal. Chem. 2019, 91, 7139−7144

pubs.acs.org/ac

Microfluidic Mixing Injector Holder Enables Routine Structural Enzymology Measurements with Mix-and-Inject Serial Crystallography Using X-ray Free Electron Lasers

George D. Calvey,[†] Andrea M. Katz,[†] and Lois Pollack*

School of Applied and Engineering Physics, Cornell University, Ithaca, New York 14853, United States

Supporting Information

ABSTRACT: The emerging technique of Mix-and-Inject Serial Crystallography (MISC) at X-ray free electron laser sources provides atomically detailed structural information about biomolecules as they function. Despite early successes, MISC is currently limited by the efficiency and robustness of the mixing injectors used to initiate the reaction and propel the sample into the X-ray beam for measurement. Here, we present a new method for fabricating the injector system that leads to simpler, faster, and more effective experiments. A mixing injector can now be produced from raw components in 100 min, only 5 min of which must be spent during the experiment, saving valuable time. The system is modular, enabling parts to be quickly exchanged in the event of unanticipated experimental difficulties, such as clogging. The injector holder is designed to be flexible, allowing each device to be optimized to maximize the number of diffraction patterns measured during each experiment. This holder has been used successfully during four beamtimes at two different X-ray free electron laser sources. Its robustness and ease of use is an important step toward making the MISC technique accessible and routine.

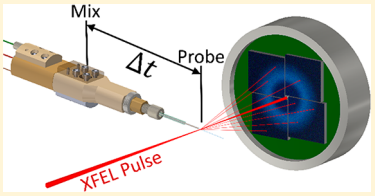

As a result of extraordinary X-ray pulse power and high repetition rates, the newest X-ray free electron laser (XFEL) sources present unmatched opportunities to advance our understanding of structural biology. XFEL sources uniquely enable room temperature crystallographic studies of micron-sized crystals, which are too small for study at traditional synchrotron sources. This developing field is called serial femtosecond crystallography (SFX).[1,2] Mix-and-inject serial crystallography (MISC) advances SFX from static to time-resolved experiments, by rapidly triggering reactions and observing biological macromolecules as they carry out their functions. Reactions are followed with atomic detail. Figure 1a) shows a schematic of a MISC experiment. A specialized device, a mixing injector, rapidly combines biological microcrystals with a reactant shortly before injection into the XFEL beam. The mixture can be probed at various time delays to measure the structure of intermediate states.[3] Early MISC experiments have provided insight into the function of both RNA and protein enzymes.[4−6] Future experiments have great potential to increase our understanding of fundamental and applied biological processes, seeding the pipeline with structures that inform our understanding of the origins and treatment of disease.

The success of a MISC experiment depends on the reliability and efficiency of the injector that mixes and dispenses the sample. Mixing injectors are, by nature, more complex than those used for standard SFX experiments. They must therefore be carefully designed to be robust and simple to operate.

Most of the currently available mixing injectors extend the capabilities of standard SFX injectors, Gas Dynamic Virtual Nozzles (GDVNs).[7] In a GDVN, a simple glass capillary tube carries the solution of microcrystals. This capillary tube is held at the center of a larger glass nozzle, through which helium gas flows. Crystal-containing solution leaves the capillary and is accelerated by a helium gas stream through the nozzle aperture to form a thin, free liquid jet.

This device can be easily modified to trigger and monitor mixing reactions by incorporating a hydrodynamic focusing mixer upstream of the helium nozzle. Within a hydrodynamic focusing device, a stream of sample solution travels into the center of a reactant solution flow.[8] The outer (reactant) solution focuses the inner (sample) solution into a thin jet which travels down the middle of the channel. The small lateral dimension of this jet allows reactant to quickly diffuse across the sample stream, initiating the reaction. This method has been successfully employed in time-resolved synchrotron X-ray scattering experiments as well as optical studies.[9−12] For a more detailed discussion of hydrodynamic mixing, see the Supporting Information (SI).

The earliest design for a MISC injector, developed by Wang and co-workers,[13] combined hydrodynamic focusing with GDVNs. In this device, a second capillary tube was placed within the GDVN to allow separate yet concentric flow of crystals, reactant, and helium. In this design, the innermost tube carries the sample solution and terminates just above the exit of the device. Here the sample emerges and is focused by the outer reactant stream to allow diffusion of reactant into the sample. This device required extremely low sample flow rates,

Received: January 17, 2019
Accepted: May 7, 2019
Published: May 7, 2019

DOI: 10.1021/acs.analchem.9b00311
Anal. Chem. 2019, 91, 7139−7144

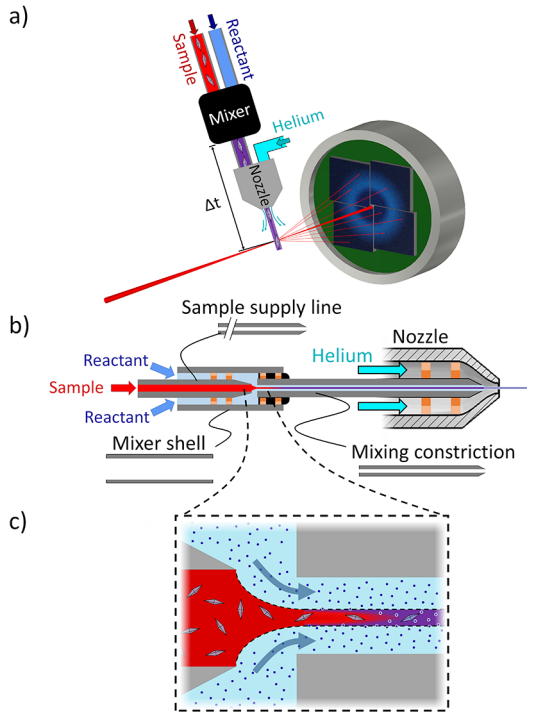

Figure 1. MISC and mixing injector overview. a) MISC experiment schematic. b) Mixing injector schematic with centering spacers shown in orange and UV curable epoxy in black. c) Cartoon close-up of the focusing region, showing diffusion of reactant across the crystal-containing jet. Blue arrows show the direction of reactant solution flow.

which would have decreased the signal acquisition rate, and was never implemented at an XFEL.

We subsequently developed a new mixing injector[14] that improved upon this prototype. Figure 1b) shows a schematic of this device. Crystals and reactant flow concentrically down two glass capillary tubes before being combined into a single outlet with a reduced diameter, the mixing constriction, as shown in Figure 1c). Within this constriction, higher flow rates of crystals can be focused into the thin jet required for mixing. This increased flow rate typically results in a rate of data acquisition and experimental efficiency comparable to a standard GDVN.[14] After a time-delay determined by the length and diameter of the constriction as well as the flow rate of the solutions, the mixture is injected into the X-ray beam for structural analysis.

This device provided access to structural dynamics on time scales orders of magnitude shorter than reported in previous XFEL experiments.[4,5] Measurement times ranging from tens of ms to several s were easily accessed and reported in studies probing the neutralization of the antibiotic ceftriaxone by β-lactamase.[6] This injector was reasonably efficient, allowing the collection of nine complete data sets during a five day beamtime. Despite these successes, several challenges were encountered. As with a standard GDVN, the capillary supply lines used to transport crystals from their reservoir to the injector must have small inner diameter to reduce their volume and the risk of crystal settling. These small diameter supply lines, however, are susceptible to clogging by clumps of crystals, shutting down the experiment. The original mixing injector device had a monolithic design with sample supply lines permanently bonded to the injector, and therefore a clog in the supply lines required replacement of the entire device. This time-consuming procedure can lead to significant amounts of experimental downtime. Because XFEL beamtime is scarce and short in duration, reducing this downtime is a high priority. Additionally, the original fabrication process included intricate and challenging steps that could only be performed by trained experts.

Here, we present the design for a new microfluidic holder that vastly simplifies the fabrication and operation of our mixing injector, greatly increasing its robustness and efficiency. This holder screws together with standard fasteners and facilitates rapid, modular assembly of the injector with detachable supply lines. With this design, it is possible to construct and assemble a fully functional, tested device in under 100 min. This modular assembly also allows portions of the mixing injector to be rapidly exchanged in the event of a clog, saving valuable experimental time. Furthermore, the holder design can accommodate a series of different mixer geometries, allowing us to optimize a given injector for a particular sample and time point. It is compatible with standard SFX beamlines and has been used successfully during four XFEL beamtimes, both at the CXI beamline at LCLS and the SPB/SFX beamline at EuXFEL. With this holder, MISC is more accessible and routine.

INJECTOR HOLDER DESIGN

The holder must provide a strong, protective housing for the mixer and nozzle, while simultaneously merging the crystal, reactant, and helium streams into concentric flows.

A CAD rendering of the holder is shown in Figure 2, along with an exploded view. It is composed of seven custom

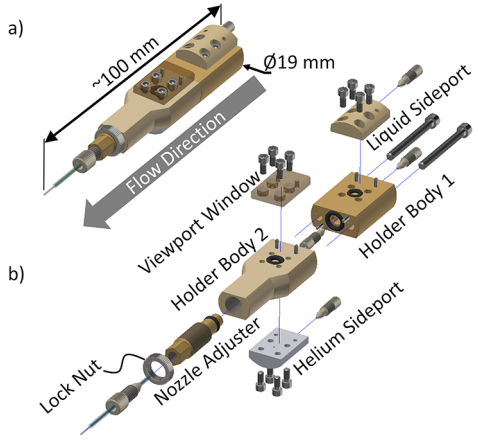

Figure 2. CAD representation of new holder, a) in its entirety and b) exploded view with custom parts labeled. Produced with Autodesk Inventor Professional 2018.

components (see SI for part drawings). All components that come into contact with liquids are made from PEEK plastic which has high chemical compatibility. O-rings form seals between the separate components of the holder and are leak-tested to at least 1500 PSI for the liquid seals and 500 PSI for the helium seals (the limits of our fluid delivery systems). Capillary connections to the holder are made with standard 6−32 and 10−32 coned fittings (Microtight and Nanotight, IDEX Health and Science, Oak Harbor, WA), allowing routine supply line changes and connections. The dimensions of the

DOI: 10.1021/acs.analchem.9b00311
Anal. Chem. 2019, 91, 7139−7144

holder were chosen to ensure compatibility with the sample environments at SFX beamlines at LCLS and EuXFEL.

At the upstream end of the device, Holder Body 1 serves as the mounting point for the mixer body and sample supply line. Connected to Holder Body 1 is the Liquid Sideport, which provides an attachment point for the reactant supply line. This upstream portion of the holder allows the substrate flow to coaxially surround the sample supply line as both enter the mixer body. Downstream, Holder Body 2 is coupled to the Helium Sideport for helium gas supply. In this portion of the device, the helium flows concentrically around the outside of the mixer and into the nozzle.

Holder Body 2 is also the attachment point for a polycarbonate Viewport Window, as well as the Nozzle Adjuster. The Viewport Window allows for easy inspection of the focusing region in longer mixing injectors. The Nozzle Adjuster facilitates rapid optimization of the nozzle geometry (and therefore the jetting behavior) by adjusting the distance between the mixer and nozzle aperture.

Figure 3a) shows a schematic view and cross section of the holder to further emphasize the roles of the various components. The sample, reactant, and helium flow paths are detailed in Figures 3b)−d), respectively. See SI for full CAD assembly and part drawings.

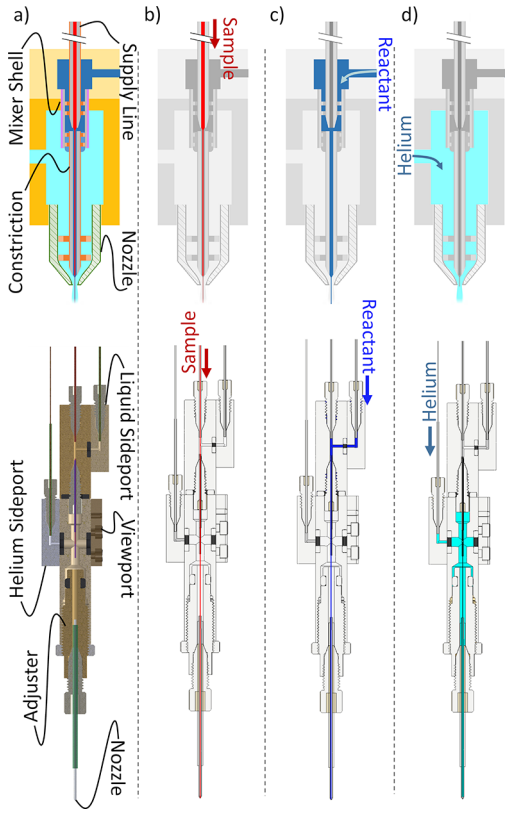

Figure 3. Overview of the new holder. a) Conceptual schematic (top) and CAD cross section (bottom). b) Sample flow path shown in red. c) Reactant flow path shown in blue. d) Helium flow path shown in cyan.

METHODS

Simplified Mixer Fabrication for Use with Microfluidic Holder. A significant advantage of this microfluidic holder is that it simplifies the fabrication and assembly of the mixer relative to the procedure described by Calvey et al.[14] This robust, simplified capillary mixer can be fabricated in almost any lab, and does not require cleanroom facilities. A summary of the mixer fabrication steps is shown in Figure 4, and a detailed list of materials and fabrication protocol is provided in the SI. The numbers listed in Figure 4 reference steps in this protocol.

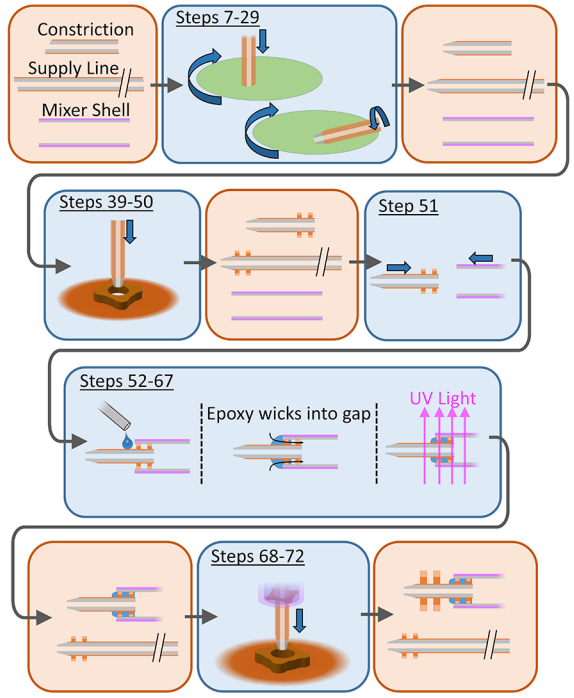

Figure 4. Cartoon of mixer fabrication process. Blue squares represent fabrication processes. The corresponding step numbers are indicated (see SI for details). Ochre squares show the state of the components following the last process step. Polishing wheels are shown in green, polyimide (coating, sheets, and spacers) is shown in orange, UV transparent coating is shown in lavender, and UV curable epoxy is shown in blue.

The first step in mixer fabrication is to cut the capillaries that will form the crystal supply line, mixing constriction, and mixer shell to length (steps 1−6). The supply line and constriction are made from standard, polyimide-coated fused silica tubing (Polymicro) with 150 or 200 μm outer diameter, and inner diameters of 30, 40, 50, 75, or 100 μm depending on the time point of interest. The mixer shell is cut from 320 μm ID/530 μm OD UV transparent tubing (Polymicro).

Once the capillaries are cut to length, both ends of the constriction and one end of the supply line are polished flat using an Allied Multiprep polishing wheel (Allied High Tech) in steps 7−19. Then, one end of the supply line and constriction are beveled to a sharp point on the same polishing wheel in steps 20−29. The bevel on the tip of the supply line helps achieve rapid and smooth flow focusing of the crystals into the constriction without creating recirculating flow; similarly, the bevel on the end of the constriction is a necessity for proper jetting out of the nozzle. Next, the constriction and supply line are each outfitted with chemically resistant polyimide centering spacers as described by Calvey et al.[14] and detailed in steps 39−50. The spacers hold the constriction and supply line concentric within the mixer body, creating very centered flows. This centering is important to minimize timing

DOI: 10.1021/acs.analchem.9b00311
Anal. Chem. 2019, 91, 7139−7144

dispersion due to the parabolic flow velocity profile inside the cylindrical capillary.

After the spacers are installed, the flat end of the constriction is inserted into the mixer shell and bonded in place with UV curable epoxy (UV15, Masterbond, steps 51−67, see SI for a schematic of our UV curing station). Then, additional spacers are placed on the end of the constriction to provide centering within the nozzle upon assembly to the full mixing injector (steps 68−72). The capillaries in this stage of assembly are shown in the last panel of Figure 4. For the remainder of this article, the constriction bonded inside of the mixer shell will be referred to as the "mixer body."

Nozzle Fabrication. The nozzle fabrication procedures are the same as for a standard GDVN[7] and are summarized in Figure 5. Briefly, a borosilicate tube (either 550 μm ID, 800 μm OD, Drummond Scientific, or 750 μm ID, 1000 μm OD, Sutter Instrument) is rotated concentrically as it is heated to melt the tip and create a small aperture (steps 81−85). See SI for a discussion of nozzle aperture sizing. After flame polishing, the nozzle is then ground down to reduce the length of the aperture (steps 86−90), which reduces debris accumulation, and beveled to remove excess glass, which can shadow the X-ray diffraction at high angles (steps 91−95).

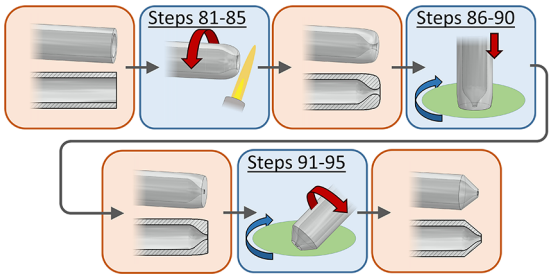

Figure 5. Nozzle fabrication process.

Injector Assembly. An overview of the assembly of a mixing injector in this holder is shown in Figure 6. First, the Liquid Side Port is attached to Holder Body 1 (step 97). Then, the tip of the crystal supply line is fed through Holder Body 1 until both spacers are visible. It is temporarily secured with a 6−32 Microtight fitting (steps 100−102). The mixer body is installed over the supply line and secured in place on the opposite end of Holder Body 1 (steps 103−106). Next, Holder Body 2 (with attached Viewport Window) is guided over the end of the mixer and attached to Holder Body 1 with a gastight O-ring seal (step 107). Following this step, the Nozzle Adjuster is threaded into Holder Body 2. The nozzle is slipped over the mixer body, and then secured in place in the Nozzle Adjuster (steps 108−110). The Lock Nut is added to prevent accidental motion of the Nozzle Adjuster (step 111). Finally, the Helium Side Port is secured to the outside of the holder and the reactant and helium supply lines are connected (steps 113−115).

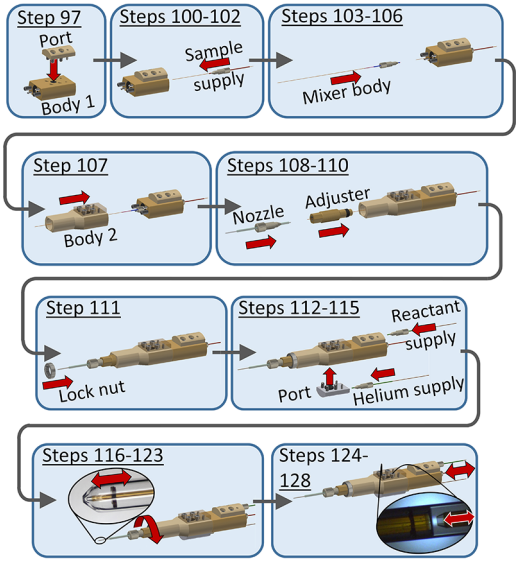

Figure 6. CAD depiction of injector assembly process in the new holder. Inset images show the constriction tip and focusing region of an actual injector after optimization.

The complete injector must be adjusted to optimize jetting. The Nozzle Adjuster can be used to vary the position of the nozzle tip relative to the end of the constriction to achieve a straight, stable jet (steps 116−123). The injector must also be adjusted to achieve the proper spacing between the supply line and the constriction in the mixer focusing region, 50 to 75 μm. The supply line can be loosened from the back of Holder Body 1 and its position tweaked by hand until the proper gap is achieved (steps 124−128).

Mounting the Injector for a MISC Experiment. The injector mounting varies depending on the hardware constraints of the XFEL beamline that the experiment will be performed at. The holder design is compatible with the standard configuration vacuum sample environments used at both CXI (LCLS) and SFX/SPB (EuXFEL), two SFX beamlines, and is easy to interface with helium and air environments found, for example, at SACLA's DAPHNIS chamber.[15] See Figure S1 for a conceptual schematic of an SFX sample environment and further information about mounting injectors for experiments at both CXI (LCLS) and SFX/SPB (EuXFEL).

RESULTS AND DISCUSSION

Efficiency of Fabrication and Operation. The new holder offers significant time savings in both the fabrication and experimental stages of a MISC experiment. The total fabrication time is reduced by about 30%. However, the time spent at the experiment preparing the injector to be loaded into the XFEL sample chamber is reduced by a factor of 7, from 36 min to just 5 min. See SI and Figure S2 for a detailed description of the XFEL sample chamber and injector preparation/loading process. Over the course of a multiple day beamtime with (potentially) several injector changes per day, this adds up to a large time savings. A detailed breakdown of fabrication time for both the original device and injectors assembled in the new holder is provided in the SI.

Another benefit of the simplified assembly protocol is the increased yield when building a batch of devices. Injectors fabricated with the new protocol and assembled in the holders have nearly a 100% success rate due to the decreased number of bonding steps and ability to repolish individual capillaries if needed.

The modular nature of the holder also reduces the risk of clogging before and during the experiment. In previous versions of the device, particulates were often introduced to the outer supply line in the process of assembling the lines coaxially. These coaxial lines are more time-consuming and

DOI: 10.1021/acs.analchem.9b00311
Anal. Chem. 2019, 91, 7139−7144

challenging to clean, and failure to remove all particulates increased the risk of clogging during the experiment. The new holder, with its noncoaxial supply lines, removes this risk and the associated time-consuming cleaning.

Increased Hit Rate. Of great concern in any SFX experiment is the crystal hit rate, defined to be the fraction of XFEL pulses which hit a crystal and result in a diffraction pattern. Because the microcrystals are randomly oriented, tens of thousands of individual patterns may be needed to solve a single structure. High hit rates reduce the amount of time needed to collect each structure, making the best use of valuable XFEL beamtime. This is especially important for a MISC experiment, where it is necessary to collect multiple data sets (time points) for each sample.

For most samples, i.e., crystals with length scales on the order of the free jet size, the hit rate in a MISC experiment is proportional to the sample flow rate.[14] Therefore, when selecting flow parameters, it is advantageous to keep the sample flow rate as high as possible. However, as the sample flow rate is increased relative to the reactant flow rate, the sample jet increases in diameter, causing an increase in mixing time (the spread in age of the sample when mixing is complete, see SI for more details). Therefore, we must carefully consider the trade-off between fast mixing and high hit rate.

To achieve the highest possible hit rate, we collect data for each time point near the maximum permissible total flow rate (limited by practical capacities of the XFEL sample environment to about 100 μL/min), which allows the highest sample flow for a given mixing time. Injectors built with small inner diameter constrictions allow faster mixing times at higher sample-to-reactant flow ratios, further increasing the achievable hit rate. The highest hit rate will therefore always be obtained by using the maximum total flow through the smallest constriction diameter possible, as determined by the clogging risk for the sample and the longest constriction length allowed by the holder.

The need for long constrictions presents a practical challenge for MISC experiments. Both ends of the constriction need to be visible in the assembled injector to check for debris and to optimize the nozzle for a straight, stable jet. Previously, this was accomplished by housing the entire constriction within the glass GDVN nozzle, where it could be easily observed. However, for long constrictions, the glass nozzles were impractically long and fragile. These factors limited the length of constriction that could be used to less than ~50 mm, and in turn, put a cap on the achievable hit rate.

The new holder's Viewport Window reduces these limitations by allowing constrictions to be partially housed within the holder, shortening the required length of the nozzle while still providing for essential observation and adjustment of the focusing region. This feature of the new holder allows the use of constrictions twice as long as previously possible (100 mm vs 50 mm), and therefore affords the option to use smaller constrictions for the same time point, providing a boost in hit rate.

Figure 7 illustrates the ability of the new holder to utilize higher sample flow rates (therefore increasing the hit rate). This figure shows the sample flow vs time point for the extended range of possible constriction lengths; the range of the old device is shown in red, and the additional range enabled by the new holder is shown in blue. This figure is based on calculations for a fixed total flow rate of 70 μL/min. For each condition, the mixing time is set to 10% of the time point; the sample flow rate varies accordingly. (In an actual SFX experiment, the choice of mixing time depends on the sample's kinetics. Here, the value of 10% was chosen to represent a case which requires relatively fast mixing.) For a given time point, the new holder supports the use of smaller diameter tubing and higher sample flow, which results in a higher hit rate. For example, acquiring a 50 ms time point in the older system required the use of a 75 μm constriction, and a sample flow rate of ~4.5 μL/min. With the new holder, this time point can be reached with a 50 μm constriction and a sample flow rate of ~10 μL/min, representing a 2.2-fold increase in hit rate. The experimental acquisition time becomes less than half of what was previously necessary.

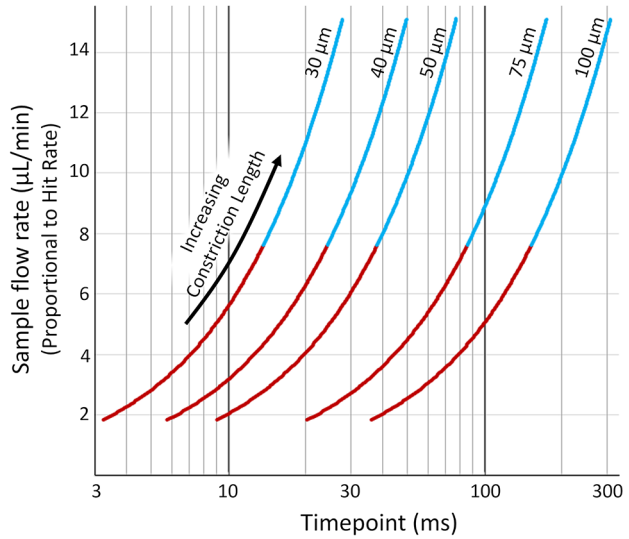

Figure 7. Plot of sample flow rate (which is usually proportional to hit rate) vs time point across the range of possible constriction lengths for various constriction diameters at fixed total flow. The red portions of the curves represent time points and flow rates achievable with the old design (constriction lengths up to 50 mm), while the blue portions show the additional range available with the new design (lengths up to 100 mm). These calculations assume a reactant diffusion coefficient of 6×10^{-10} m^2/s, and a mixing threshold of 30%. (See SI for a detailed explanation of mixing times and thresholds.)

While the new holder allows significant gains, there is a practical limit on mixing time and hit rate imposed by the particular crystals for an experiment. To avoid clogging, the largest dimension of the crystal should be less than the diameter of the constriction. In addition, the smallest dimension of the crystals sets a lower limit on the size of the focused jet (and therefore an upper limit on the mixing time), since the reducing the jet beyond this crystal dimension will not significantly reduce the time needed for reactant to soak into the crystals. Currently, there is not a general method for measuring soaking times into microcrystals; however, the diffusion coefficient in crystals is lower than in solution.[16]

CONCLUSIONS

The new microfluidic holder presented here increases the efficiency and robustness of XFEL mixing injectors, reducing the required assembly time during beamtime by a factor of 7. It is easy to assemble and use, both because of its modular, screw together design, and because the supply lines can be attached independently with standard fittings. The Viewport Window permits the use of long constrictions without dangerously long,

DOI: 10.1021/acs.analchem.9b00311
Anal. Chem. 2019, 91, 7139−7144

unsupported nozzles, allowing experiments to proceed with increased hit rate to better utilize precious XFEL beamtime. It has proven valuable at experiments at both CXI (LCLS) and SPB/SFX (EuXFEL) beamlines, and represents a step forward in making MISC an accessible and routine technique.

■ ASSOCIATED CONTENT

Supporting Information

The Supporting Information is available free of charge on the ACS Publications website at DOI: 10.1021/acs.analchem.9b00311.

Additional information on the XFEL sample environment, how to mount a mixing injector, full assembly protocol, mixing theory/terminology, and a detailed guide to designing a mixing injector (PDF)

Technical drawings for mixing injector holder assembly and EuXFEL nozzle rod (detailed part and assembly drawings) (PDF)

■ AUTHOR INFORMATION

Corresponding Author

*E-mail: lp26@cornell.edu.

ORCID

Lois Pollack: 0000-0002-9366-4396

Author Contributions

†These authors contributed equally.

Notes

The authors declare no competing financial interest.

■ ACKNOWLEDGMENTS

We thank Nathan Ellis for advice and guidance on the design and machining of the microfluidic holders. This work was funded by NSF Science and Technology Center Grant No. 1231306.

■ REFERENCES

(1) Schlichting, I. *IUCrJ* **2015**, *2* (2), 246−255.

(2) Boutet, S.; Lomb, L.; Williams, G. J.; Barends, T. R.; Aquila, A.; Doak, R. B.; Weierstall, U.; DePonte, D. P.; Steinbrener, J.; Shoeman, R. L.; et al. *Science* **2012**, *337* (6092), 362−364.

(3) Schmidt, M. *Adv. Condens. Matter Phys.* **2013**, *2013*, 1−10.

(4) Stagno, J. R.; Liu, Y.; Bhandari, Y. R.; Conrad, C. E.; Panja, S.; Swain, M.; Fan, L.; Nelson, G.; Li, C.; Wendel, D. R.; et al. *Nature* **2017**, *541* (7636), 242−246.

(5) Kupitz, C.; Olmos, J. L.; Holl, M.; Tremblay, L.; Pande, K.; Pandey, S.; Oberthür, D.; Hunter, M.; Liang, M.; Aquila, A.; et al. *Struct. Dyn.* **2017**, *4* (4), 044003.

(6) Olmos, J. L., Jr; Pandey, S.; Martin-garcia, J. M.; Calvey, G.; Katz, A.; Knoska, J.; Kupitz, C.; Hunter, M. S.; Liang, M.; Oberthuer, D.; et al. *BMC Biol.* **2018**, *16* (59), 1−15.

(7) DePonte, D. P.; Weierstall, U.; Schmidt, K.; Warner, J.; Starodub, D.; Spence, J. C. H.; Doak, R. B. *J. Phys. D: Appl. Phys.* **2008**, *41* (19), 195505.

(8) Knight, J.; Vishwanath, A.; Brody, J.; Austin, R. *Phys. Rev. Lett.* **1998**, *80* (17), 3863−3866.

(9) Pollack, L.; Tate, M. W.; Darnton, N. C.; Knight, J. B.; Gruner, S. M.; Eaton, W. A.; Austin, R. H. *Proc. Natl. Acad. Sci. U. S. A.* **1999**, *96* (18), 10115−10117.

(10) Russell, R.; Millett, I. S.; Tate, M. W.; Kwok, L. W.; Nakatani, B.; Gruner, S. M.; Mochrie, S. G. J.; Pande, V.; Doniach, S.; Herschlag, D.; et al. *Proc. Natl. Acad. Sci. U. S. A.* **2002**, *99* (7), 4266−4271.

(11) Dootz, R.; Otten, A.; Koster, S.; Struth, B.; Pfohl, T. *J. Phys.: Condens. Matter* **2006**, *18*, S639.

(12) Park, H. Y.; Kim, S. A.; Korlach, J.; Rhoades, E.; Kwok, L. W.; Zipfel, W. R.; Waxham, M. N.; Webb, W. W.; Pollack, L. *Proc. Natl. Acad. Sci. U. S. A.* **2008**, *105* (2), 542−547.

(13) Wang, D.; Weierstall, U.; Pollack, L.; Spence, J. C. H. *J. Synchrotron Radiat.* **2014**, *21*, 1364−1366.

(14) Calvey, G. D.; Katz, A. M.; Schaffer, C. B.; Pollack, L. *Struct. Dyn.* **2016**, *3*, 054301.

(15) Tono, K.; Nango, E.; Sugahara, M.; Song, C.; Park, J.; Tanaka, T.; Tanaka, R.; Joti, Y.; Kameshima, T.; Ono, S.; et al. *J. Synchrotron Radiat.* **2015**, *22*, 532−537.

(16) Geremia, S.; Campagnolo, M.; Demitri, N.; Johnson, L. N. *Structure* **2006**, *14* (3), 393−400.

DOI: 10.1021/acs.analchem.9b00311
Anal. Chem. 2019, 91, 7139−7144